Volume 1 | Number 1 | Jan 2013 | Pages 1–100

PCCP

Physical Chemistry Chemical Physics
www.rsc.org/pccp

ROYAL SOCIETY OF CHEMISTRY

ROYAL SOCIETY OF CHEMISTRY

www.rsc.org/pccp

^{13}C NMR Investigations and Molecular Order of
4-(trans-4'-hexylcyclohexyl)-isothiocyanatobenzene (6CHBT)

Nitin P. Lobo[a], B. V. N. Phani Kumar[a], T. Narasimhaswamy[b], and Asit Baran Mandal[a,b,c]*

[a]*Chemical Physics Laboratory,* [b]*Polymer Laboratory and* [c]*Chemical Laboratory*
Council of Scientific and Industrial Research (CSIR)-Central Leather Research Institute
(CLRI), Chennai 600020, Adyar, India.

[*]Corresponding author. E-mail: abmandal@hotmail.com, abmandal@clri.res.in
(A. B. Mandal), Fax : +91-44-24912150, Tel.:+91-44-24910846/0897

Abstract

The static 1D ^{13}C and 2D Proton Encoded Local Field (PELF) NMR experiments are carried out in the nematic phase of a low viscous liquid crystal 4-(trans-4'-hexylcyclohexyl)-isothiocyanatobenzene (6CHBT) with a view to find orientational order. The PELF spectra provide better resolution which facilitates the assignment of cyclohexyl and phenyl ring carbons relatively easy. For the cyclohexyl unit, four pairs of dipolar splitting are clearly noticed in contrast to earlier reports for structurally similar mesogens where only two pairs of doublets are seen. The linear relation between anisotropic chemical shifts and orientational order are established and semi-empirical parameters are obtained to aid the study of the order behaviour of 6CHBT over the entire nematic range. The data further fitted to the Haller equation and a reasonable good agreement is observed. The temperature dependence trends of orientational order parameters extracted for various carbons using ^{13}C-^{1}H dipolar couplings with those of ^{13}C chemical shifts are compared. A gradual decrease in order parameter is noticed for different molecular segments while traversing from core to aliphatic

chain via cyclohexyl ring. The notable decreasing trends of order parameters along the chain are observed similar to those of the corresponding phenyl cyclohexanes reported earlier.

Keywords: ^{13}C NMR, ^{13}C-^{1}H dipolar couplings, order parameter, 6CHBT, PELF

1. Introducton

Thermotropic liquid crystals exhibiting nematic mesophase often consist of two rings in the core along with terminal chains as well as other units.[1] Among them, MBBA and 5CB are constructed with phenyl rings in the core either with alkyl chains as terminal units or other moieties.[2] The salient features of these nematogens are that they exhibit low transition temperatures and hence, are widely used both for applications as well as for fundamental research studies.[2] Yet another class of nematogens which gained immense popularity due to interesting physicochemical properties are those based on phenyl cyclohexanes.[3] These are usually constructed with phenyl ring directly linked to cyclohexane as a core with flexible terminal chains and polar units. Further, these mesogens are found to be chemically stable, exhibit low melting temperature as well as colorless thus finding applications in display devices. Dabrowski had extensively carried out the physicochemical properties of phenyl cylcohexanes with reference to influence of terminal chains/units.[4] For instance, the presence of isothiocyanate at the terminal position in phenyl cyclohexane is known to reduce the bulk viscosity as well as bend elastic constant of the nematogens. Similarly, the dielectric anisotropy is found to be lower for nematogens in which isothiocyanate is at one end of the core. In view of these interesting properties, one of the mesogen, which belongs to phenyl cyclohexane family possessing a terminal isothiocyanate commonly known as 4-trans-4'-hexylcylcohexyl)-isothocyanatobenzene (6CHBT) achieved significant popularity.[4-6] The liquid crystal 6CHBT is a low viscous and low melting mesogen with a nematic phase over a wide temperature range. It is often used as a base component of many mixtures operating at

low temperatures in the twisted nematic as well as super twisted nematic configurations.[4] The synthesis of 6CHBT was described [5] and its physiochemical properties are thoroughly examined.[6] The earlier studies dealing with dielectric and viscosity measurements on 6CHBT provided information on molecular rotation around the short axis.[7] Similarly, the strength of the nematic potential as well as the effective length of the 6CHBT molecule in the isotropic phase are also investigated.[8] ^{1}H NMR relaxometry investigations on short-range nematic order and order director fluctuations in isotropic as well as nematic phases of 6CHBT yielded fruitful information on molecular dynamics and their correlation with underlying structure in terms of correlation times and activation energies.[9] Very recently, the influence of the alkyl chain length on spectral and photorefractive properties of liquid crystals from the CHBT family in the terahertz range are also carried out.[10]

NMR spectroscopy is the most powerful experimental tool to study the orientational order at the atomistic level, which is the hallmark of liquid crystals.[11,12] In recent years, ^{13}C NMR spectroscopy has attained significant importance as it provides atomistic information for mesogens in their mesophase.[13-17] With the advent of 2D Separated Local Field (SLF) experiments,[18] the ^{13}C NMR techniques achieved greater prominence for probing the molecular dynamics as well as molecular order.[19-21] However, most of the ^{13}C NMR studies reported in literature deals mainly with those mesogens in which core is mostly constructed with phenyl rings. To the best our knowledge, the ^{13}C NMR studies of phenyl cyclohexanes, on the other hand, are very limited despite their immense popularity.[22] Hence, in the present work, we report the variable-temperature ^{13}C NMR and 2D Proton Encoded Local Field (PELF) [23] investigations in the nematic phase of 6CHBT with a view to extract information on orientational order from ^{13}C chemical shifts and [13]C-^{1}H dipolar couplings, which will stimulate further studies.

2. Experimental

High purity commercial grade 6CHBT and solvent $CDCl_3$ were obtained from Sigma Aldrich, USA. The compound 6CHBT was used without further purification. The T_{NI} (43°C) and T_{CN} (12°C) are temperatures of transition between nematic to isotropic and crystalline to nematic phase respectively are determined from optical polarizing microscope or shortening of NMR FID.

Solid state NMR: The solid-state NMR experiments were performed on a Bruker Avance-III-HD 400 WB NMR spectrometer (9.4 T). The proton and carbon resonance frequencies were 400.07 and 100.61 MHz, respectively. The spectra in the nematic phase of the sample were recorded in the range between 16 and 42°C using a double resonance 4 mm MAS probe under static condition. The sample was aligned by first heating to the isotropic phase and then slowly cooling to the mesophase for NMR measurements. The ^{13}C NMR spectra in the nematic phase were obtained by using a standard cross-polarization pulse scheme with a contact time of 3ms following the 90° proton pulse width of 4 μs. SPINAL-64[24] decoupling was employed during carbon signal acquisition using a proton decoupling strength of 30 kHz. To avoid sample heating, the recycle delay between each FID was kept as 12s and each spectrum was obtained with 96 scans.

Two-dimensional high resolution SLF spectra were obtained in the mesophase under static condition by using PELF technique as shown in Figure S1 of Electronic Supplementary Information (ESI) that correlates the ^{13}C chemical shift with the associated ^{13}C-^1H dipolar couplings. Application of PELF pulse sequence to liquid crystalline systems has been reported in detail in earlier publications.[25-27] During t_1 period, BLEW-48[28] homonuclear decoupling sequence was employed with a r. f. power of 71.4 kHz and a 30 kHz SPINAL-64 heteronuclear decoupling was used during t_2 period. Ramp CP scheme was used as a magnetization transfer step with a ramped contact pulse of 1.5 ms. Typically, 24 transients

4

were used for each t_1 period with a recycle delay of 25 s between scans to avoid sample

heating and 128 t_1 increments were employed. The 2D data matrix was double Fourier

transformed with 256 and 4k points in F_1 and F_2 dimensions, respectively and processed in

phase sensitive mode with shifted square sine bell apodization used in the F_1 dimension. The

F_1 dimension frequency axis was scaled with a scaling factor of 0.42. For the evaluation of

scaling factor, we recorded the 1D fully proton coupled ^{13}C spectrum of ^{13}C labelled

chloroform oriented in the nematic liquid crystal 4- n- pentyl- 4'-cyanobiphenyl (5CB) and

also the 2D-PELF spectrum of the same sample. The ^{13}C-^1H splitting obtained in the former

experiment was used to estimate the scaling factor for the latter.

3. Results and Discussion

The molecular structure of 6CHBT is shown in Figure 1. It consists of two rings in the

core which is directly linked. Further, the hexyl chain connected to cyclohexyl ring and

isothiocyanate bonded to phenyl ring serve as terminal groups. The Figure 1 also shows the

numbering of the core as well as terminal chain carbons. The ^{13}C NMR measurements are

carried out in the nematic phase with a view to extract the orientational order parameters for

various carbons.

The chemical shift assignment of all the carbons of the mesogen in solution is very crucial

for the assignment of chemical shift in nematic phase. The molecular structure of the

mesogen in solution is carried out by various 1D and 2D experiments, viz. ^1H, ^{13}C, DQF

COSY, HMBC and INADEQUATE. Since the mesogen consists of cyclohexyl ring, which

exists in chair conformation, the assignment of proton as well as carbon signals is very

essential prior to the investigation of ^{13}C chemical shifts in mesophase. The ^{13}C solution

NMR spectrum of 6CHBT is depicted in Figure 2A and the line assignments are discussed in

detail in ESI. Table 1 lists the ^1H and ^{13}C solution chemical shift values. The complete

structural assignment of the molecule is in consistent with the similar mesogens earlier reported by Fung and co-workers.[29]

The mesogen exhibits nematic phase in the range 12 - 43°C. The static ^{13}C NMR spectrum measured at 20°C is shown in the Figure 2B. Well resolved sharp lines of the spectrum indicate the orientation of the mesogen in the magnetic field. The assignment of carbons in nematic case has been carried out by following the solution spectral assignment. The spectrum in the region 150 - 202 ppm shows 4 lines with different intensity. Two lines appeared with comparable intensity in the region 150 - 153 ppm are assigned to phenyl ring carbons, whereas low intense broad peak centered at 186.6 ppm is attributed to quaternary carbon of phenyl ring to which NCS is attached. The other quaternary carbon is noticed at 201.3 ppm with an observable intensity. For cyclohexyl as well as hexyl chain, a group of lines are observed in the range 13 - 40 ppm. The terminal methyl is assigned to 13.2 ppm while carbon 1 is assigned to 39.3 ppm. The comparison of ^{13}C chemical shift values of static spectrum with the solution spectrum (Figure 2) clearly indicates the alignment of the molecule in nematic phase. Series of 1D spectra were also recorded in the range of temperature from 16 to 42°C and some of them are shown in the Figure 3 for clarity. For phenyl ring carbons, an increase in chemical shift values is noticed, whereas for cyclohexyl ring and hexyl chain, decrease in chemical shifts is observed. These changes indicate parallel alignment of the molecule with respect to magnetic field. Furthermore, the appearance of two lines for aromatic methine carbons indicates π flips of the ring with respect to local axis (C$_2$ axis). The alignment induced chemical shift (AIS) values determined by δ_{lc} - δ_{soln} are listed in Table 2, where AIS trends support the parallel alignment of the molecule with respect to magnetic field. The interesting feature of the spectrum is observation of intense sharp line at 33.2 ppm, which is attributed to both the methylene carbons (2, 3, 5, 6) of cyclohexyl ring. In solution NMR, the chemical shift difference between carbons 2, 6 and 3, 5 is found to be less

than ~1 ppm, whereas in static spectrum superimposition of them is clearly seen. As a consequence of the above, the number of ^{13}C resonance lines is found to be 9 instead of 10, while moving to nematic phase from isotropic one, as evident from Figure 2.

The 2D PELF experiments of the mesogen were carried out in nematic phase at four different temperatures to measure the [13]C-^{1}H dipolar couplings with a view to extract the orientational order parameters. The PELF spectrum provides correlation between ^{13}C chemical shifts (ppm) and the corresponding [13]C−[1]H dipolar couplings (kHz) depicted, respectively along the F_2 and F_1 dimensions. A typical spectrum obtained at 20°C is shown in Figure 4A. Well resolved sharp contours were observed and their respective dipolar slices provide high resolution information (Figure 4B). The cross-sections for all the carbon resonances show either one or two pairs of outer lines which correspond to the short-range interactions between protons and carbons resulting in large dipolar splitting. A group of lines at the centre is due to the long-range interactions resulting in smaller splitting. The [13]C-^{1}H dipolar coupling constant (D_{CH}) is related to the observed splitting Δv by the following equation

$$\Delta v = f\,(2D_{CH} + J_{CH}) \tag{1}$$

where f is a scaling factor (0.42) for the homonuclear decoupling sequence (BLEW-48) and J_{CH} is the scalar coupling constant. The J_{CH} values for directly bonded CH pairs were measured from 1D proton coupled ^{13}C NMR spectrum of 6CHBT in $CDCl_3$ which are listed in Table 1. As noted from earlier reports,[22, 26] the sign of the dipolar couplings cannot be determined experimentally. However, for directly bonded CH pairs, based on geometric considerations, the sign can be assigned as positive. For phenyl ring the 2' carbon shows two doublets, where the outer dipolar splitting correspond to the directly bonded CH pair and the inner splitting is due to non-bonded CH pair. In the case of carbon 3', these two splittings are very similar in magnitude and hence unresolved in the 2D spectrum. The quaternary carbons

couple to two identical ortho protons and give rise to a pair of dipolar splitting among which

signal for 4' carbon is found to be low intense. The interesting feature of the spectrum is for

cyclohexyl ring for which four pair of dipolar splittings are observed for 2, 3, 5, 6 carbons

centred at 33.2 ppm. In earlier studies, Fung et al. observed only two pairs of doublets and the

long range couplings were not properly resolved.[22,26] Here the largest ^{13}C-^{1}H dipolar coupling

6.24 kHz arises from axial protons and 3.03 kHz due to equatorial protons. Among remaining

two pair of doublets, the 1.30 kHz and 0.71 kHz couplings arise from long range couplings,

which are tentatively assigned to axial and equatorial protons, respectively. This observation

is further confirmed by looking at the 1 and 4 carbons of cyclohexyl ring, which shows

doublet with a largest coupling in the range of 6.2 - 6.4 kHz due to axial protons and a

moderately resolved smaller doublet arises from long range coupling. This is based on the

fact that 1 and 4 carbons are connected to phenyl ring and hexyl chain, respectively. As a

result, one proton is directly attached to carbon (methine). Since the trans geometry for 1, 4-

disubstituted cyclohexane demands location of bulkier substituents at the equatorial position,

the lone proton is seen at the axial position. Since the ^{13}C-^{1}H dipolar coupling values of 1 and

4 are exclusively contributed by axial protons, the ^{13}C-^{1}H dipolar couplings are direct

reflection of axial contribution. Table 2 lists the ^{13}C-^{1}H dipolar couplings of all the carbon

resonances of the mesogen in the nematic phase at four temperatures i.e., 20°C, 28°C, 32°C

and 40°C. For the terminal hexyl chain, every carbon shows a doublet due to splitting by the

directly bonded protons and also shows small dipolar doublets arising from nearby protons.

At higher temperatures some of the long range couplings are not resolved due to smaller

values. The large ^{13}C-^{1}H dipolar coupling value of 5.73 kHz facilitated the assignment of α

carbon. For ω carbon, high intense dipolar doublet is noticed with a smaller splitting.

From the experimental dipolar couplings obtained from the PELF experiment, the local

order parameters $S_{zz'}$ and $(S_{xx'} - S_{yy'})$ of the phenyl ring can be determined. Since the phenyl

ring undergoes π flips, the D_2 symmetry is assumed for the phenyl ring. The ^{13}C-^{1}H dipolar couplings are employed in order to extract the orientational order parameter by making use of following equation[11,15,16]

$$D_{CH} = K\{½ (3 \cos^2\theta_{z'} - 1) S_{zz'} + ½ (\cos^2\theta_{x'} - \cos^2\theta_{y'})(S_{xx'} - S_{yy'})\} \quad (2)$$

where $K = -h\gamma_H\gamma_C/4\pi^2 r^3_{CH}$, with γ_H and γ_C are respectively the gyromagnetic ratios of hydrogen and carbon nuclei, r_{CH} is the distance between the carbon and hydrogen nuclei and $\theta_{x'}, \theta_{y'}$ and $\theta_{z'}$ are angles between r_{CH} vector and the coordinate axes. Accordingly, the C_2 axis is taken as z'-axis while y'-axis is the in-plane axis perpendicular to z'. For calculating K in equation (2), standard bond distances, namely 1.1 Å for the C–H bond and 1.4 Å for the C–C bond, are taken. Also during fitting, the two C–C–H bond angles are varied slightly around 120°(an ideal hexagonal geometry) due to the uncertainty involved in the position of the H atom as determined by X-rays.[30] The $S_{zz'}$ and $(S_{xx'} - S_{yy'})$ for the phenyl ring calculated at different temperatures are listed in Table 3.

For cyclohexyl ring due to C_{2h} or C_s symmetry three order parameters are required to find the orientational ordering. However, if there is a distortion of the perfect chair conformation, the symmetry can be reduced to C_i. The earlier investigations showed that axial CH bonds are not strictly parallel to each other in the structurally similar mesogens.[22] As the data available is not sufficient to determine all three order parameters for C_s symmetry, the S_{xy} value is assumed to be zero. Based on the axis system shown in Figure 5 the S_{zz} and $(S_{xx} - S_{yy})$ for cyclohexyl ring are determined by the following equations:[22]

$$S_{zz} = 1/K \{ D_{CH}(a) + \sec^2(\theta - 90) D_{CH}(e)\} \quad (3)$$

and

$$(S_{xx} - S_{yy}) = 1/K \{D_{CH}(a) - \sec^2(\theta - 90) D_{CH}(e)\} \quad (4)$$

Where a = axial, e = equatorial, and θ is the H-C-H bond angle and taken as $\theta=107.5°$.[31] For the order parameter calculation, only directly bonded couplings are considered and the

corresponding order parameter values are listed in Table 4. The calculated order parameter values for cyclohexyl ring are comparable with the structurally similar systems reported earlier.[22] For terminal hexyl chain due to the presence of large number of segmental motions, finding the exact orientational ordering is challenging. This problem can be circumvented by assuming an axial symmetry for CH bond. Then, the order parameter for the CH bond is directly related to the corresponding CH dipolar coupling by[16]

$$S_{CH} = 1/K \{ D_{CH} \} \tag{5}$$

Accordingly, the CH_2 as well as CH_3 order parameters measured at four temperatures are also listed in Table 4. It is clear from the Table that the phenyl ring shows high $S_{zz'}$ values in contrast to cyclohexyl ring (S_{zz}). This suggests that for phenyl ring is more rigid than cyclohexyl ring. The ($S_{xx} - S_{yy}$) values, on the other hand, are found to be higher for cyclohexyl than phenyl ring. With the increase in temperature, a decrease in order parameter value is noticed, which is consistent with the nematic mesophase behaviour.[19,21] In the case of terminal chain, the order parameter values decrease along the chain and the same trend is followed at all temperatures. This behaviour is in consistent with those based on phenyl cyclohexanes that are reported earlier.[22] It is interesting, however, to note that this is in contrast to the trend observed for terminal chains in which an alternation of order parameter for CH carbons is generally seen.[32]

The validity of order parameters obtained from ^{13}C-^1H dipolar couplings is further verified by measuring the ^{13}C chemical shifts using 1D static experiment at different temperatures. This facilitates to examine the behaviour of order parameters over a wide nematic range. The 2D PELF experiments were performed at four different temperatures, viz. 20, 28, 32 and 40°C and the corresponding order parameters at these temperatures are estimated by using ^{13}C-^1H dipolar couplings. These order parameter can be related to the ^{13}C chemical shifts through a semi-empirical equation by adopting the established protocols[33,34]

$$\Delta\delta \approx aS + b \tag{6}$$

where $\Delta\delta = \delta_{lc} - \delta_{iso}$ is AIS, a and b are semi empirical constants. For a 1,4- disubstituted phenyl ring the two-fold para axis is taken as the z axis and for an axially symetric CH bonds in the aliphatic chains, the CH axis is approximated as the z axis. Accordingly, the subscript zz is dropped in equation (6). Often it is noticed that for phenyl ring as well as terminal aliphatic chain, the $(S_{xx} - S_{yy})$ are very small and the values are temperature independent. In the case of cyclohexyl ring, both S_{zz} and $(S_{xx} - S_{yy})$ show systematic dependence on temperature. Hence the equation (6) is considered strictly as an empirical manner for both the order parameters. The values of $\Delta\delta$ for each of the carbon resonances at four different temperatures were then plotted against the order parameters. The values of a and b along with errors and correlation coefficient (R^2) obtained from linear least-squares fitting for phenyl ring, hexyl chain and cyclohexyl ring respectively are listed in Tables 5 and 6. The high correlation coefficients (R^2) suggest good linearity for all the carbons across the measured nematic range. By utilizing a and b values, the order parameters of all the segments for other temperatures can be calculated easily from ^{13}C chemical shifts alone. Figure 6 shows the corresponding S plots for phenyl and aliphatic chain carbons while for cyclohexyl ring, both the order parameters i.e. S_{zz} and $(S_{xx} - S_{yy})$ are shown. This data is further fitted to the Haller equation, which describes the temperature dependence of order parameter as [33,35]

$$S(T) = S_0 (1-T/T^*)^F \tag{7}$$

where S_0 and F are empirical constants and T^* is a temperature at which the order parameter becomes zero. Initially T^* was used as a variable to fit to equation (7) for each curve and the average value of 319.6 K was used as a fixed parameter for final fitting. The solid curves in the Figure 6 are obtained by fitting the order parameter calculated from chemical shifts to the Haller equation and the obtained S_0 and F are tabulated in Table 7. The plot supports a good agreement between experimental and the order parameter values extracted from Haller

equation. Further, these values are in well agreement with those computed from [13]C-^{1}H dipolar couplings measured from 2D experiments. Thus the investigation reveals that the combination of 2D PELF and 1D ^{13}C chemical shift measurements can provide better insight in to the ordering of different segments of the mesogen across the mesophase range.

4. Conclusion

A combined study of static 1D ^{13}C NMR as well as 2D PELF experiments were performed on the nematogen 6CHBT. The orientational order parameters for various molecular segments of the mesogen were determined by using [13]C-^{1}H dipolar couplings and further corroborated by the ^{13}C chemical shifts measured over a broad nematic range. The analysis revealed a good linearity between chemical shifts and order parameters, which facilitates to study the temperature dependence of the order parameters over a wide temperature range using AIS. The order parameter values of phenyl (0.60) and cyclohexyl (0.422) rings at 20˚C indicates higher order for phenyl ring, which is attributed to higher rigidity of phenyl ring as against cyclohexyl ring of the core unit. An increase in the order parameter value was seen for different molecular segments while going from aliphatic chain to core via cyclohexyl ring. A general trend of decrease in the order parameter along the chain was noticed and it further supports the alike behavior observed for structurally similar types of mesogens investigated earlier.[22] As the study clearly demonstrated the high resolution structure for cyclohexane ring where long range couplings are well resolved (four pairs of doublets) in nematic mesophase, whereas earlier studies showed only two pairs of dipolar splittings.[22] It is anticipated that such a high resolution NMR studies of mesogens involving cyclohexane may stimulate interest since low temperature nematogens are important for display applications.

Acknowledgment

References

(1) S. Chandrasekhar, *Liquid Crystals*, Cambridge University Press, Cambridge, 1992; P. J. Collings and M. Hird, *Introduction to Liquid Crystals Chemistry and Physics,* Taylor and Francis, London, 1997; G. R. Luckhurst and G. W. Gray, *The Molecular Physics of Liquid Crystals*, Academic Press, New York, 1979; A. D. Demus *in Handbook of Liquid Crystals*, Vol.1 (Eds: D. Demus, J. W. Goodby, G. W. Gray, H. W. Spiess and V. Vill), WILEY-VCH, Weinhiem, Germany, 1998, pp. 133−187.

(2) I. -C. Khoo, *Liquid Crystals*, John Wiley & Sons, Inc., New Jersey, 2007; D. Yang and S. Wu, *Fundamentals of Liquid Crystal Devices*, John Wiley & Sons Ltd, Chichester, 2006.

(3) M. Petrzilka, *Mol. Cryst. Liq. Cryst.*, 1985, **131**, 109-123.

(4) R. Dabrowski, *Mol. Cryst. Liq. Cryst.*, 1990, **191**, 17-27.

(5) J. W. Baran, Z. Raszewski, R. Dabrowski, J. Kedzierski and J. Rutkowska, *Mol. Cryst. Liq. Cryst.*, 1985, **123**, 237-245.

(6) P. Sarkar, P. Mandal, S. Paul, S.; R. Paul, R. Dabrowski and K. Czuprynski, *Liq. Cryst.*, 2003, **30**, 507-527.

(7) J. Jadzyn, L. Hellemans, G. Czechowski, C. Legrand and R. Douali, R. *Liq. Cryst.*, 2000, **27**, 613-619.

(8) R. B. Bogoslovov, C. M. Roland, J. Czub and S. Urban, *J. Phys. Chem. B*, 2008, **112**, 16008-16011.

(9) B. V. N. Phani Kumar, V. Satheesh, K. Venu and V. S. S. Sastry, *Phase Transit.*, 2009, **82**, 131-145.

(10) U. Chodorowa, J. Parka and K. Garbat, *Liq. Cryst.* 2013, **40**, 1089-1094.

(11) J. W. Emsley and J. C. Lindon, *NMR Spectroscopy Using Liquid Crystal Solvents*, Pergamon Press, Oxford, 1975.

(12) M. Cifelli, V. Domenici and C. A. Veracini, *Curr. Opin. Colloid Interface Sci.*, 2013, **18**, 190-200.

(13) A. Ramamoorthy, ed. *Thermotropic Liquid Crystals: Recent Advances*, Springer: Dordrecht, The Netherlands, 2007.

(14) R. Y. Dong, *Nuclear Magnetic Resonance Spectroscopy of Liquid Crystals*, World Scientific, Singapore, 2009.

(15) B. M. Fung, *Prog. Nucl. Magn. Reson. Spectrosc.*, 2002, **41**, 171−186.

(16) B. M. Fung, *Encyclopedia of Magnetic Resonance*, 1996, **4**, 2744−2751.

(17) R. Y. Dong and A. Marini, *J. Phys. Chem. B*, 2009, **113**, 14062−14072; R. Y. Dong, A. Marini, V. Hamplova, M. Kaspar, and C. A. Veracini, *J. Phys. Chem. B*, 2007, **111**, 9787−9794.

(18) R. K. Hester, J. L. Ackerman, V. R. Cross and J. S. Waugh, *Phys. Rev. Lett.*, 1975, **34**, 993–995.; J. S. Waugh, *Proc. Natl. Acad. Sci. U.S.A.*, 1976, **73**, 1394–1397.

(19) J. Xu, K. Fodor-Csorba and R. Y. Dong, *J. Phys. Chem. A*, 2005, **109**, 1998−2005.

(20) T. Narasimhaswamy, D. K. Lee, K. Yamamoto, N. Somanathan and A. Ramamoorthy, *J. Am. Chem. Soc.*, 2005, **127**, 6958−6959; T. Narasimhaswamy, M. Monette, D. K. Lee and A. Ramamoorthy, *J. Phys. Chem. B*, 2005, **109**, 19696−19703.

(21) S. Kalaivani, T. Narasimhaswamy, B. B. Das, N. P. Lobo and K. V. Ramanathan, *J. Phys. Chem. B*, 2011, **115**, 11554−11565; N. P. Lobo, M. Prakash, T. Narasimhaswamy and K. V. Ramanathan, *J. Phys. Chem. A*, 2012, **116**, 7508−7515; M. K. Reddy, K. S. Reddy, K. Yoga, M. Prakash, T. Narasimhaswamy, A. B. Mandal, N. P. Lobo, K. V. Ramanathan, D. S. S. Rao and K. S. Prasad, *J. Phys. Chem. B*, 2013, **117**, 5718-5729; M. K. Reddy, K. S. Reddy, T. Narasimhaswamy, B. B. Das, N. P. Lobo and K. V. Ramanathan, *New J. Chem.*, 2013, **37**, 3195-3206.

(22) C. B. Frech, B. M. Fung and M. Schadt, *Liq. Cryst.*, 1988, **3**, 713-722; C. B. Frech, B. M. Fung and M. Schadt, *Proc. SPIE*, 1989, **1080**, 215-226.

(23) M. Hong, A. Pines and S. Caldarelli, *J. Phys. Chem.*, 1996, **100**, 14815-14822; S. Caldarelli, M. Hong, L. Emsley and A. Pines, *J. Phys. Chem.*, 1996, **100**, 18696-18701.

(24) B. M. Fung, A. K. Khitrin and K. Ermolaev, *J. Magn. Reson.*, 2000, **142**, 97−101.

(25) S. V. Dvinskikh, H. Zimmermann, A. Maliniak and D. Sandstrom, *J. Magn. Reson.*, 2003, **163**, 46–55.

(26) C. Tan and B. M. Fung, *J. Phys. Chem. B.*, 2003, **107**, 5787-5790; J. W. Emsley, P. Lesot, G. D. Luca, A. Lesage, D. Merlet and G. Pileio, *Liq. Cryst.*, 2008, **35**, 443-464; L. Beguin, J. W. Emsley, M. Lelli, A. Lesage, G. R. Luckhurst, B. A. Timimi and H. Zimmermann, *J. Phys. Chem. B.*, 2012, **116**, 7940-7951. , J. W. Emsley, M. Lelli, A. Lesage and G. R. Luckhurst, *J. Phys. Chem. B.*, 2013, **117**, 6547-6557.

(27) H. Sun, M. D. Roth and B. M. Fung, *Liq. Cryst.*, 2001, **28**, 1469-1474.

(28) D. P. Burum, N. Linder and R. R. Ernst, *J. Magn. Reson.*, 1981, **44**, 173-188.

(29) C. B. Frech, B. M. Fung and M. Schadt, *Magn. Reson. Chem.*, 1988, **26**, 433-435.

(30) B. M. Fung, J. Afzal, T. L. Foss and M. –H. Chau, *J. Chem. Phys.*, 1986, **85**, 4808−4814.

(31) O. Bastiansen, L. Fernholt, H. M. Seip, H. Kambara and K. Kuchitsu, *J. Mol. Struct.*, 1973, **18**, 163-168.

(32) P. Forster and B. M. Fung, *J. Chem. Soc., Faraday Trans. 2*, 1988, **84**, 1083-1094.

(33) W. Guo and B. M. Fung, *J. Chem. Phys.*, 1991, **95**, 3917-3923.

(34) T.-H. Tong, J. P. Bayle and B. M. Fung, *Liq. Cryst.*, 1997, **22**, 165-169.

(35) I. Haller, *Prog. Solid State Chem.*, 1975, **10**, 103-118.

Table 1: ^{1}H, ^{13}C chemical shifts and scalar couplings (J_{CH}) of 6CHBT mesogen in the solution state at room temperature. Here *a* means axial and *e* means equatorial protons.

C. No	1'	2'	3'	4'	1	2,6	3,5	4	α	β	γ	δ	ε	ω	NCS
^{1}H (ppm)	-	7.16	7.14	-	2.44	1.84(e), 1.38(a)	1.86(e), 1.04(a)	1.21	1.23	1.3	1.27	1.29	1.24	0.88	-
^{13}C (ppm)	147.3	127.8	125.5	128.5	44.2	34.1	33.4	37.1	37.3	26.9	29.6	31.9	22.7	14.1	134.4
J_{CH} (Hz)	-	160.5	163.5	-	125.4	126.8	124.8	122.4	124.8	126.5	125.6	123.9	124.7	124.4	-

Table 2: ^{13}C chemical shifts (CS), anisotropy induced shifts (AIS) and corresponding dipolar couplings (D_{CH}) ^{a} of 6CHBT mesogen in nematic phase at four temperatures.

| Carbon No.	Nematic phase											
	20 °C			28 °C			32 °C			40 °C		
	CS (ppm)	AIS (ppm)	D_{CH}^{b} (kHz)	CS (ppm)	AIS (ppm)	D_{CH}^{b} (kHz)	CS (ppm)	AIS (ppm)	D_{CH}^{b} (kHz)	CS (ppm)	AIS (ppm)	D_{CH}^{b} (kHz)
1'	201.3	54.0	0.77	198.9	51.6	0.70	195.7	48.4	0.66	187.9	40.6	0.54
2'	152.1	24.3	1.73 -1.24	151.1	23.3	1.57 -1.18	149.8	22.0	1.45 -1.15	146.5	18.7	1.18 0.96
3'	150.3	24.8	1.30 -1.30	149.2	23.7	1.18 -1.18	147.8	22.3	1.11 -1.11	144.4	18.9	0.90 -0.90
4'	186.6	58.1	0.79	184.2	55.7	0.73	180.5	52.0	0.67	172.4	43.9	0.57
1	39.3	-4.9	6.25 0.80	39.5	-4.7	5.82 0.73	39.9	-4.3	5.39 0.71	40.7	-3.5	4.55 0.59
2, 3, 5, 6 (a)^c	33.2	-0.9	6.24 1.30	33.3	-0.8	5.71 1.21	33.3	-0.8	5.42 1.15	33.5	-0.6	4.51 0.98
2, 3, 5, 6 (e)^d	33.2	-0.2	3.03 0.71	33.3	-0.1	2.84 0.66	33.3	-0.1	2.70 0.62	33.5	0.1	2.27 0.51
4	35.7	-1.4	6.35 0.79	35.7	-1.4	5.89 0.75	35.9	-1.2	5.45 0.69	36.2	-0.9	4.56 0.58
α	24.4	-12.9	5.73 0.50	25.2	-12.1	5.22 0.44	26.3	-11.0	5.09 0.41	28	-9.3	4.23 0.34
β	20.8	-6.1	4.89 0.59	21.1	-5.8	4.42 0.53	21.6	-5.3	4.16 0.50	22.7	-4.2	3.44 0.41
γ	23.3	-6.3	4.85 0.32	23.7	-5.9	4.39 0.28	24.2	-5.4	4.06	25.4	-4.2	3.39
δ	25.3	-6.6	3.73 0.46	25.7	-6.2	3.34 0.42	26.3	-5.6	3.11 0.39	27.5	-4.4	2.49 0.31
ε	19.9	-2.8	3.54 0.30	20.2	-2.5	3.16	20.5	-2.2	2.91	21.1	-1.6	2.34
ω	13.2	-0.9	0.24	13.3	-0.8	0.21	13.4	-0.7	0.19	13.7	-0.4	0.14

^{a} The errors for the dipolar couplings are about ±0.03 kHz.

^{b} The first entry values are coupling from directly bonded C–H pairs; the second entry values are from indirectly bonded C–H pairs. For cyclohexyl ring and aliphatic chain the indirectly bonded dipolar coupling signs undetermined.

^{c} a means dipolar coupling due to axial protons.

^{d} e means dipolar coupling due to equatorial protons.

Table 3: Orientational order parameters of phenyl ring and the corresponding calculated ^{13}C-^{1}H dipolar couplings for 6CHBT mesogen at four temperatures.
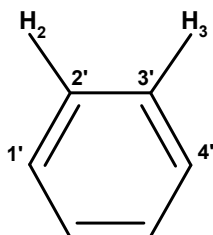
T(°C)	Angle		$S_{zz'}$	$S_{xx'}-S_{yy'}$	Calculated dipolar couplings (kHz)						RMSD (kHz)
	$\theta_{2'}$	$\theta_{3'}$			$C_{2'}$-H_2	$C_{2'}$-H_3	$C_{3'}$-H_3	$C_{3'}$-H_2	$C_{1'}$-H_2	$C_{4'}$-H_3	
20	118.4	119.7	0.60	0.058	1.68	-1.28	1.30	-1.28	0.77	0.78	0.03
28	118.4	119.8	0.56	0.054	1.55	-1.19	1.18	-1.20	0.71	0.73	0.01
32	118.5	119.8	0.52	0.050	1.43	-1.11	1.10	-1.11	0.67	0.68	0.02
40	118.6	119.8	0.43	0.041	1.17	-0.92	0.91	-0.91	0.55	0.56	0.02

Table 4: Orientational order parameters for the cyclohexyl ring and aliphatic C-H bonds of 6CHBT mesogen at four temperatures.

	20˚C		28˚C		32˚C		40˚C	
	S_{zz}	$(S_{xx} - S_{yy})$	S_{zz}	$(S_{xx} - S_{yy})$	S_{zz}	$(S_{xx} - S_{yy})$	S_{zz}	$(S_{xx} - S_{yy})$
Cyclohexane	0.422	0.128	0.389	0.114	0.370	0.108	0.309	0.089
	S_{CH}		S_{CH}		S_{CH}		S_{CH}	
α	-0.253		-0.230		-0.224		-0.186	
β	-0.216		-0.195		-0.183		-0.152	
γ	-0.214		-0.194		-0.179		-0.149	
δ	-0.164		-0.147		-0.137		-0.110	
ε	-0.156		-0.139		-0.128		-0.103	
ω	-0.011		-0.009		-0.008		-0.006	

Table 5: Semiempirical parameters along with errors and correlation coefficient (R^2) for each carbon resonances of phenyl ring and aliphatic chain obtained from relation between order parameter(S) and AIS by using equation (6)

	1'	2'	3'	4'	α	β	γ	δ	ε	ω
a	78.19	32.61	34.35	84.16	41.30	30.08	32.44	55.77	22.48	96.15
	±3.7	±1.8	±1.6	±2.9	±3.9	±1.7	±2.9	±4.5	±0.7	±16.8
b	7.18	4.77	4.21	7.91	-1.70	-0.33	0.54	1.83	0.71	0.14
	±2.0	±0.9	±0.8	±1.5	±0.9	±0.3	±0.5	±0.6	±0.1	± 0.1
R^2	0.993	0.991	0.994	0.996	0.973	0.991	0.976	0.981	0.997	0.914

Table 6: Semiempirical parameters along with errors and correlation coefficient (R^2) for each carbon resonances of cyclohexane ring obtained from relation between S_{zz} and AIS, (S_{xx} - S_{yy}) and AIS by using equation (6).

	Order parameter	1	2	3	4
a	S_{zz}	-12.64 ±0.7	-2.61 ±0.3	-2.61 ±0.3	-4.53 ±0.3
	(S_{xx} - S_{yy})	-36.73 ±4.3	-7.61 ±1.1	-7.61 ±1.1	-13.13 ±1.8
b	S_{zz}	0.38 ±0.3	0.20 ±0.1	0.90 ±0.1	0.49 ±0.1
	(S_{xx} - S_{yy})	-0.30 ±0.5	0.06 ±0.1	0.76 ±0.1	0.24 ±0.2
R^2	S_{zz}	0.990	0.955	0.955	0.984
	(S_{xx} - S_{yy})	0.960	0.937	0.937	0.948

22

Table 7: Values of S_o and F obtained by fitting the order parameters to the Haller equation.

	$S_{zz'}$	S_{zz}	$(S_{xx} - S_{yy})$	S_{CH}					
	Phenyl Ring	Cyclohexyl Ring	Cyclohexyl Ring	α	β	γ	δ	ε	ω
So	1.103	0.735	0.239	-0.432	-0.400	-0.404	-0.332	-0.323	-0.031
F	0.243	0.223	0.256	0.217	0.249	0.259	0.285	0.296	0.426

Figure Captions:

Figure 1: Molecular Structure of 4-(trans-4'-hexylcyclohexyl)-isothiocyanatobenzene (6CHBT) mesogen.

Figure 2: Proton-decoupled (A) ^{13}C NMR spectrum of 6CHBT mesogen dissolved in ^{13}CDCl$_3$ and (B) ^{13}C CP spectrum of the static oriented sample of 6CHBT at 20°C in the nematic phase.

Figure 3: ^{13}C static CP spectra of the mesogen at variable temperature range.

Figure 4: (A) ^{13}C$-^{1}$H 2D PELF spectrum of the mesogen in the nematic phase at 20°C. (B) Dipolar cross sections corresponding to all the carbon resonances of the mesogen. For 4' carbon the vertical scales for the cross-sections are indicated.

Figure 5: Representation of molecular axis for the phenyl ring (z') and cyclohexyl ring (z) moieties in 6CHBT.

Figure 6: Plot of order parameters (S) of all carbon resonances against the reduced temperature T/T*. Whereas, for cyclohexyl ring carbons both term of order parameter S_{zz} and $(S_{xx} - S_{yy})$ are plotted and marked exclusively for clear distinction. The solid lines were obtained by fitting the experimental data to the Haller equation (7).
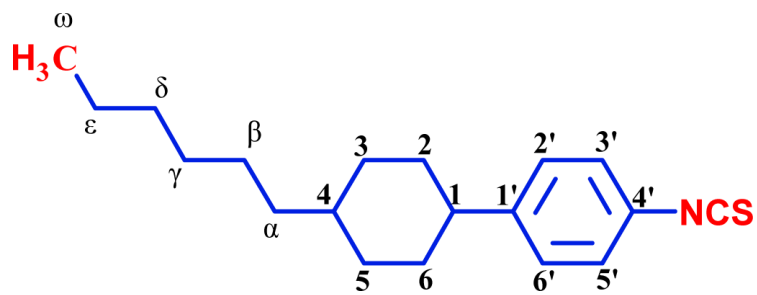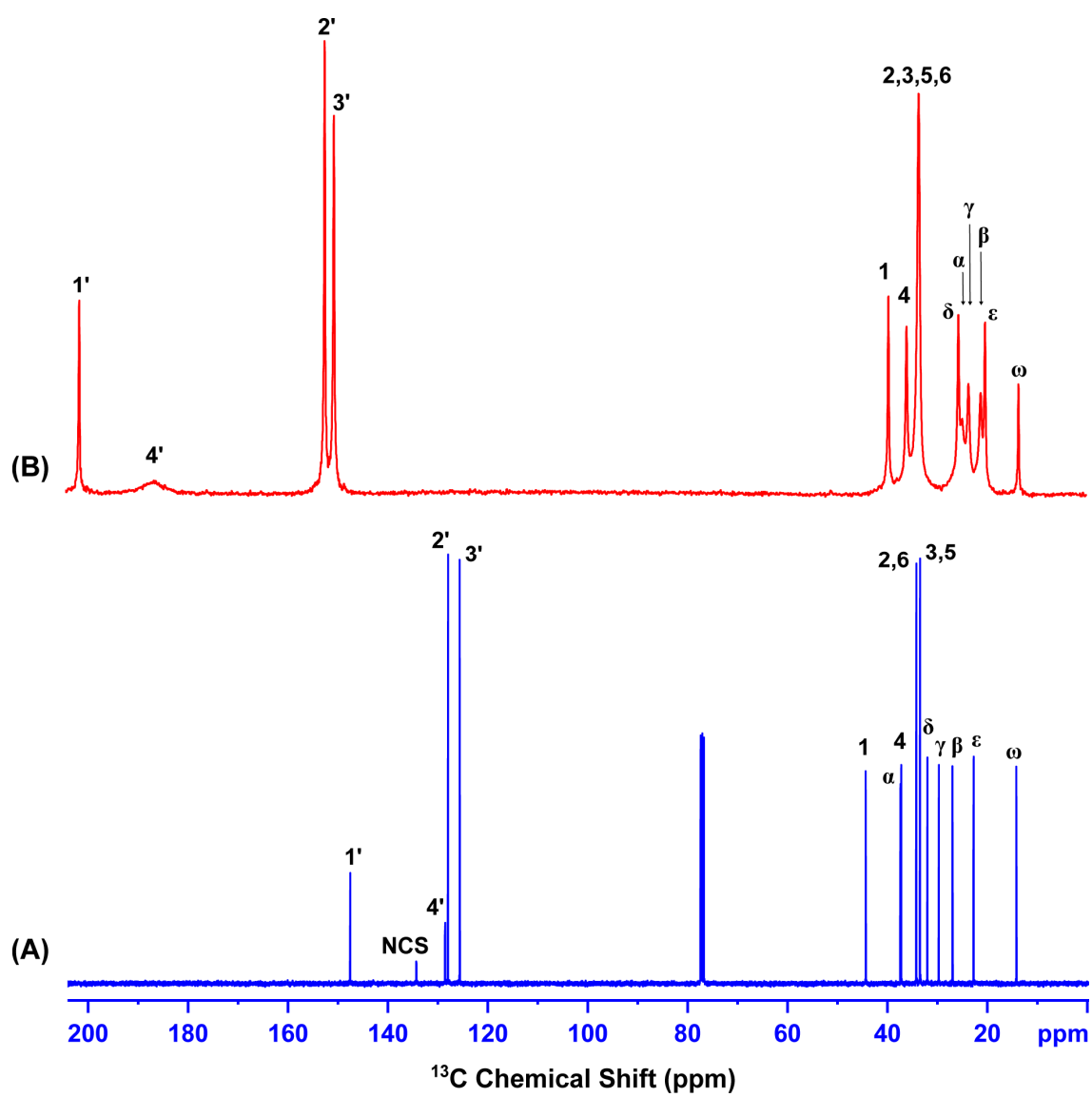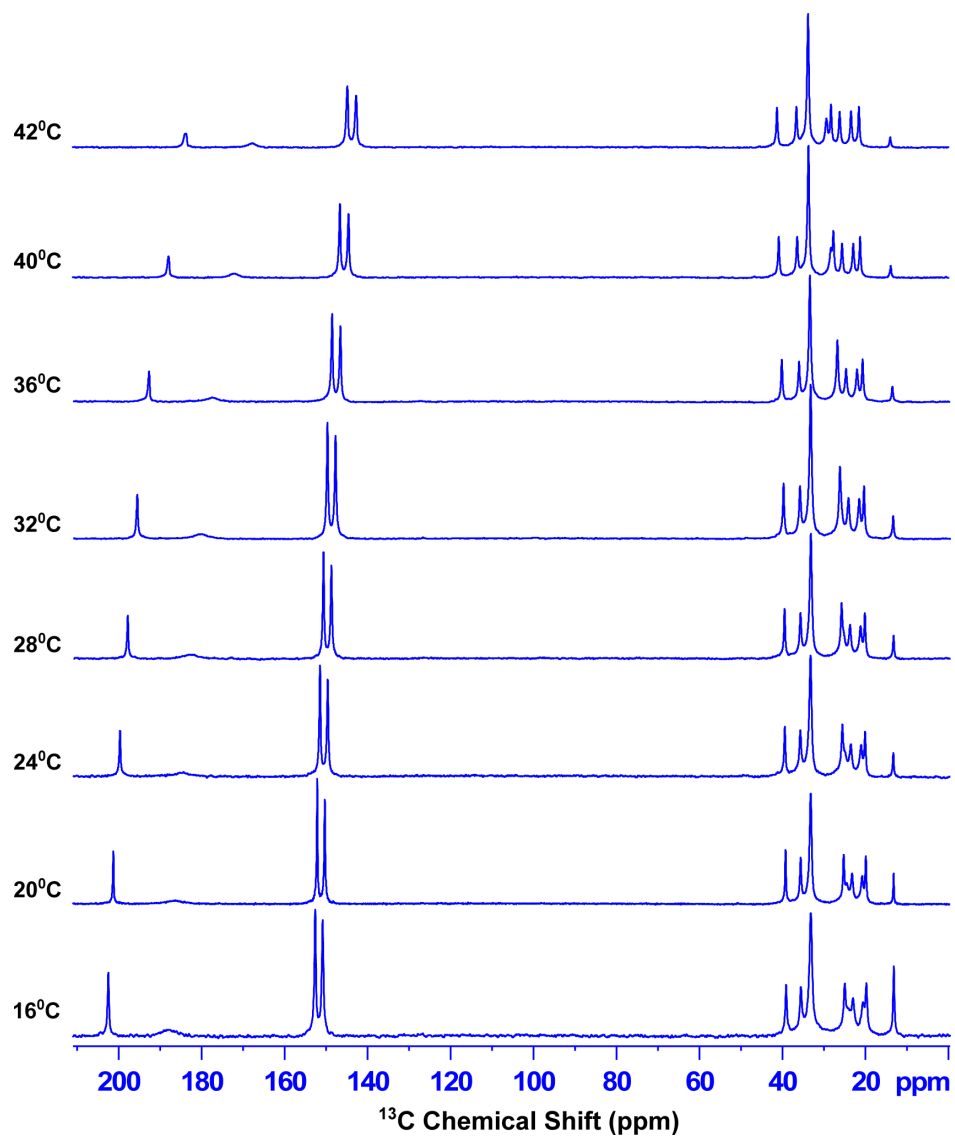
24

Figure 1

Figure 2

Figure 3

Figure 4

Figure 5

Figure 6